Unidirectional High-Power Generation via Stress-Induced Dipole Alignment from $ZnSnO_3$ Nanocubes/Polymer Hybrid Piezoelectric Nanogenerator

*Keun Young Lee, Dohwan Kim, Ju-Hyuck Lee, Tae Yun Kim, Manoj Kumar Gupta, and Sang-Woo Kim**

The extremely stable high-power generation from hybrid piezoelectric nanogenerator (HP-NG) based on a composite of single-crystalline piezoelectric perovskite zinc stannate ($ZnSnO_3$) nanocubes and polydimethylsiloxane without any electrical poling treatment is reported. The HP-NG generates large power output under only vertical compression, while there is negligible power generation with other configurations of applied strain, such as bending and folding. This unique high unidirectionality of power generation behavior of the HP-NG provides desirable features for large-area piezoelectric power generation based on vertical mechanical compression such as moving vehicles, railway transport, and human walking. The HP-NGs of $ZnSnO_3$ nanocubes exhibit high mechanical durability, excellent robustness, and high power-generation performance. A large recordable output voltage of about 20 V and an output current density value of about 1 μA cm^{-2} are successfully achived, using a single cell of HP-NG obtained under rolling of a vehicle tire.

1. Introduction

Lead-free perovskite nanostructures with high piezoelectric charge constants are attracting much attention due to their potential applications in nanosensors, actuators, energy harvesting, and piezotronics.[1–4] In recent years, energy-harvesting technologies that can scavenge various kinds of mechanical energy from the living environment have attracted increasing attention.[5–13] Environmentally friendly lead-free piezoelectric/ferroelectric materials have great potential for medical imaging and biological devices, which can be implanted directly into the human body due to their biocompatibility. However, many lead-free piezoelectric materials still remain undiscovered or require further investigation.[14]

Among such materials, zinc stannate ($ZnSnO_3$) has been a focal point of research, because it is a piezoelectric and ferroelectric material with electrical and structural ordering temperature well above room temperature, up to 700 °C.[15,16] $ZnSnO_3$ has perovskite-type and ilmenite-type structures, forming face-centered-cubic close packing.[17] $ZnSnO_3$ exhibits excellent polarization of ≈59 μC cm^{-2} along the *c*-axis, which is larger than that of other lead-free materials, such as potassium niobate ($KNbO_3$, 23 μC cm^{-2}), zinc oxide (ZnO, 5 μC cm^{-2}), and barium titanate ($BaTiO_3$, 6 μC cm^{-2}).[17–20] Furthermore, increased interest has developed around $ZnSnO_3$, because of its symmetry-dependent properties such as piezoelectricity, ferroelectricity, pyroelectricity, and second-order nonlinear optical behavior that originate from its non-centrosymmetric properties.[17] In addition, its physical properties can be modulated by controlling its morphology, dimensions, crystallinity, and preparation methods. Recently, $ZnSnO_3$ micro/nanostructures have been synthesized via various routes, including co-precipitation, thermal evaporation, and low-temperature ion exchange methods.[21–23] Semiconducting $ZnSnO_3$ nanostructures, which have a direct band gap of 1.0 eV at room temperature, have been applied as building blocks to fabricate sensors, transistors, displays, solar cells, and electrode materials for rechargeable batteries.[24–28]

Recently, polymer-mold-supporting nanogenerators (NGs) fabricated using various nanostructured piezoelectric materials like ZnO, $BaTiO_3$, $KNbO_3$, and sodium niobate ($NaNbO_3$) have been reported.[29–33] These composite-based hybrid piezoelectric NGs (HP-NGs) are very attractive for large-scale piezoelectric energy harvester applications, because of easy fabrication, cost-effectiveness, and mechanical robustness. However, the power generation using HP-NGs reported thus far are mostly feasible under bending conditions only after an electrical poling treatment[30–33] and there has been no report demonstrating high power generation from HP-NGs operated under vertical compression without any electrical poling treatment. The realization of vertical compressive-force-driven HP-NGs is desirable for large-area piezoelectric power generation using various sources of mechanical energy featuring vertical compression, such as moving vehicles, railway transport, and human walking.

K. Y. Lee, Dr. M. K. Gupta, Prof. S.-W. Kim
School of Advanced Materials Science and Engineering
Sungkyunkwan University (SKKU)
Suwon 440-746, Republic of Korea
E-mail: kimsw1@skku.edu
D. Kim, J.-H. Lee, T. Y. Kim, Prof. S.-W. Kim
Advanced Institute of Nanotechnology (SAINT)
Center for Human Interface Nanotechnology (HINT)
SKKU, Suwon 440-746, Republic of Korea

DOI: 10.1002/adfm.201301379

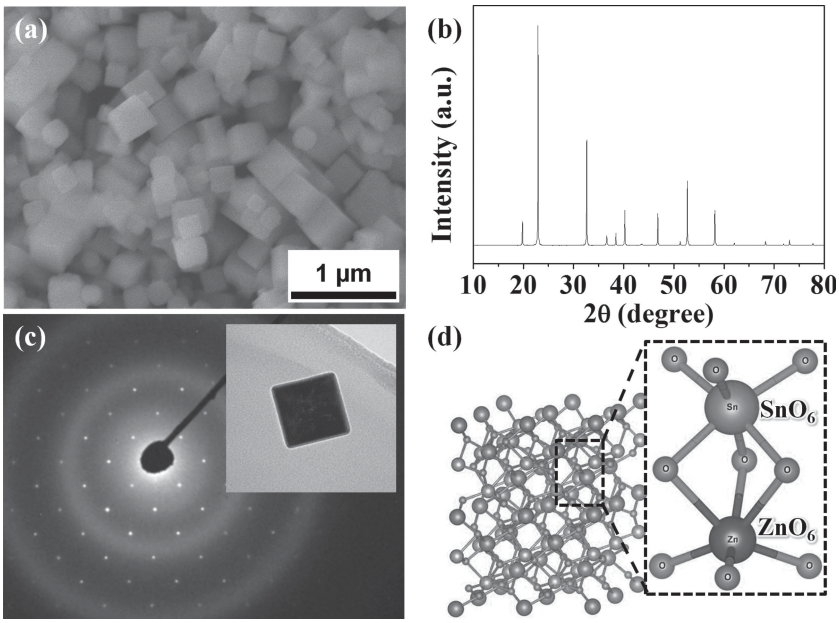

Figure 1. a) FE-SEM image of as-grown $ZnSnO_3$ nanocubes synthesized at 80 °C. b) XRD pattern of the $ZnSnO_3$ as-grown nanocubes. c) EF-TEM image of single nanocube (inset) and selected area electron diffraction pattern of the same crystal. d) Crystallographic structure of $ZnSnO_3$, showing two octahedral frameworks of ZnO_6 (lower side) and SnO_6 (upper side).

We report on extremely stable unidirectional high-power generation using HP-NGs based on single-crystalline piezoelectric perovskite $ZnSnO_3$ nanocubes and polydimethylsiloxane (PDMS) polymer without any treatment of electrical poling. The HP-NG is effectively operated under vertical compression, with negligible power generation under other configurations of strain applied, including bending and folding. This unique high unidirectionality and high power generation behavior is desirable for large-area piezoelectric power generation applications involving vertical mechanical compression. HP-NGs exhibit high mechanical durability, excellent robustness behavior, and high power-generation performance. A recordable large output voltage of about 20 V and an output current density value of about 1 μA cm^{-2} from a single HP-NG cell are successfully obtained under the rolling a vehicle tire.

2. Results and Discussion

A typical field-emission scanning electron microscopy (FE-SEM) image of the $ZnSnO_3$ nanocubes is shown in **Figure 1**a, exhibiting a well-defined cubic morphology with an edge size of about 100–200 nm. The corresponding morphologies of the $ZnSnO_3$ nanostructures synthesized at different reaction temperatures are shown in the Supporting Information, Figure S1, and reveal that the morphology and size of synthesized $ZnSnO_3$ nanostructures highly depend on the reaction temperature. With increasing reaction temperature, the morphology of $ZnSnO_3$ is converted from spherical shape to cubic shape.

The X-ray diffraction (XRD) results of the $ZnSnO_3$ nanocubes are provided in Figure 1b. The XRD pattern of the $ZnSnO_3$ nanocubes is identified according to the Joint Committee on Powder Diffraction Standards 11-0274,[15] demonstrating that perovskite-structure $ZnSnO_3$ is formed. The crystal structure of the $ZnSnO_3$ nanocubes are indexed to the rhombohedral structure of an *R3c* space group with lattice constants of $a = b = 0.526$ nm and $c = 1.400$ nm, and is grown along the [001] axis. The spectrum also indicates that the $ZnSnO_3$ nanostructure is fully crystallized, and no impure phases are observed in the sample. The XRD patterns of different $ZnSnO_3$ samples are shown in the Supporting Information, Figure S2. It is clear from the patterns that the intensity of diffraction peaks increases with increasing reaction temperature. Based on these results, $ZnSnO_3$ cubic crystallites have been selected for NG fabrication because of their larger surface area, smaller particle size, high crystallinity, and uniform morphology properties. Figure 1c shows energy-filtering transmission electron microscope (EF-TEM) image (inset) taken from a $ZnSnO_3$ single nanocube, and its corresponding selected area electron diffraction (SAED) pattern. The SAED pattern exhibits periodic diffraction spots, demonstrating the single-crystalline nature of the nanocube.

Figure 1d shows the crystallographic structure of the $ZnSnO_3$ material. $ZnSnO_3$ is based on two octahedral frameworks of ZnO_6 and SnO_6. The ZnO_6 octahedron has three short bonds of 0.2041 nm and three long bonds of 0.2308 nm. The SnO_6 octahedron has three short bonds of 0.2008 nm and three long bonds of 0.2094 nm.[17] In these unequal bond lengths between the O–Sn–O and O–Zn–O in the $ZnSnO_3$ structures, the Sn and Zn deviate from the octahedron center by nonequivalent amounts along the *c*-axis, and a Zn atom is located at a large distortion position along the *c*-axis, which results in noncentrosymmetric extended structure. Therefore, spontaneous polarization is generated along the *c*-axis, which is the source of piezoelectricity in $ZnSnO_3$.

A schematic presentation of the fabricated HP-NG based on the $ZnSnO_3$:PDMS composite structure is shown in **Figure 2**a. The HP-NG device mainly consists of four layers. The piezoelectric $ZnSnO_3$ nanocubes are homogenously mixed with PDMS and sandwiched between a gold (Au)/chromium (Cr) top electrode and an indium tin oxide (ITO) bottom electrode coated onto polyethylene naphthalate (PEN) substrate. Cross-sectional FE-SEM images (inset of Figure 2a and Supporting Information, Figure S3) obviously show that the white $ZnSnO_3$ nanocubes are randomly distributed inside the PDMS, such that the electric dipoles presented in the $ZnSnO_3$ are randomly oriented between the top and bottom electrodes.

To measure the piezoelectric power-generating performance and mechanical durability of the device, a direct impact approach was used. A heavy motor vehicle was used to apply a vertical compressive force on a large HP-NG positioned on a road. Figure 2b shows a photograph of the actual experimental setup for scavenging energy from a rolling tire due to vehicle

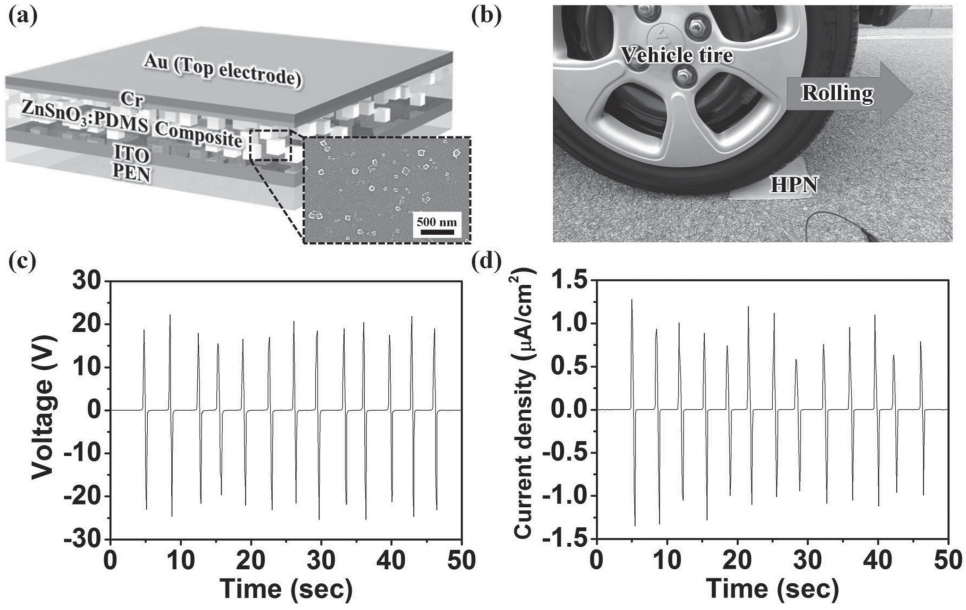

Figure 2. Structure of flexible hybrid piezoelectric nanogenerator (HP-NG) and its power generation under the rolling of a tire. a) Schematic diagram presenting the structure of the ZnSnO3:PDMS composite-based flexible HP-NG. The $ZnSnO_3$:PDMS is sandwiched between top (Au/Cr) and bottom electrodes (ITO coated PEN plastic substrate). The cross-sectional FE-SEM image shows that $ZnSnO_3$ nanocubes are randomly distributes inside the PDMS polymer. b) Original image presenting the experimental setup for power generation under the rolling of a vehicle tire, in which $ZnSnO_3$:PDMS HP-NG was attached to a road. c) Output voltage and d) current density from HP-NG induced by the loading and unloading of a vehicle tire.

motion. The observed output voltage and current from the HP-NG, which has an effective size of 10 cm × 10 cm, are given in Figures 2c,d. Power generation from HP-NG under rolling tire is also recorded and given in the Supporting Information, Video S1. A large output voltage of 20 V and current density of 1 μA cm^{-2} were obtained. This high power-generation performance is quite stable, even after 500 cycles of tire rolling. These results reveal the robustness and mechanical durability of the HP-NG, as shown in **Figure 3**a. Since the crystal structure of $ZnSnO_3$ is very stable even under very high pressure (≈21 GPa), and therefore $ZnSnO_3$ can generate a substantial piezoelectric signal.[34] For simplicity, we consider that HP-NG only experienced normal compressive stress under rolling tire due to vehicle motion, and the corresponding charge generation mechanism is discussed in detail in the next section.

Polarity-switching tests were also carried out to confirm that the output voltage originated from the piezoelectric phenomenon. An opposite output signal is observed when the device is connected in reverse connection as shown in Figure 3b. Based on these results, it can be suggested that the $ZnSnO_3$ nanocube-PDMS composite HP-NG is promising and effective for harvesting the mechanical energy from moving vehicles, as well as powering small electronic equipment beside the road, and realizing self-powered speed sensors and pressure sensors for transport monitoring.

The voltage and current outputs from the HP-NG were also investigated as a function of the force applied under vertical compression from a mechanical force stimulator (Supporting Information, Figure S4). The voltage outputs from the HP-NG (40 wt% $ZnSnO_3$) with different pushing forces are presented in **Figure 4**a, which has an effective size of 1 cm × 1 cm. Only a small enhancement was observed in the output voltage and current with increasing external vertical compressive strain up to ≈0.52% (Region I), beyond which the output voltage and current increased abruptly, reaching maximum values of about 12 V and 0.89 μA cm^{-2}, respectively, under a vertical compressive strain of 0.91% (Region II). The actual output voltage and current data are given in the Supporting Information, Figure S5. It is proposed that external strain of up to 0.52% cannot produce significant strain on a piezoelectric $ZnSnO_3$ nanocube due to the presence of PDMS which endures the majority of the strain. Therefore, only a small enhancement in the piezoelectric output signals could be observed with the HP-NG. Since the electric dipoles are randomly distributed between the electrodes, small mechanical strain cannot align the dipoles significantly. On the other hand, the piezoelectric output voltage and current density increase linearly from 4 V to 12 V and from 0.26 μA cm^{-2} to 0.89 μA cm^{-2}, respectively, with an increase of the compressive strain from 0.67% to 0.91% (Region II). It is well known that the output voltage from piezoelectric power generators increases linearly with the applied strain/stress. A larger strain of ≈0.91% leads to a higher strain inside the $ZnSnO_3$ nanocubes, which results in the generation of a stronger piezoelectric potential and higher corresponding piezoelectric signals from the HP-NG. The observed output voltage and current levels from the HP-NG in this work are very high compared to previous composite-based piezoelectric NGs.[29–33]

To investigate the effect of $ZnSnO_3$ nanocube concentration on the power generation performance of the HP-NGs, a series of HP-NGs were fabricated with different ratios of $ZnSnO_3$ and PDMS (10, 20, 40, and 60 wt% $ZnSnO_3$). We obtained piezoelectric output voltages around 2, 4, 10, and 3 V from the

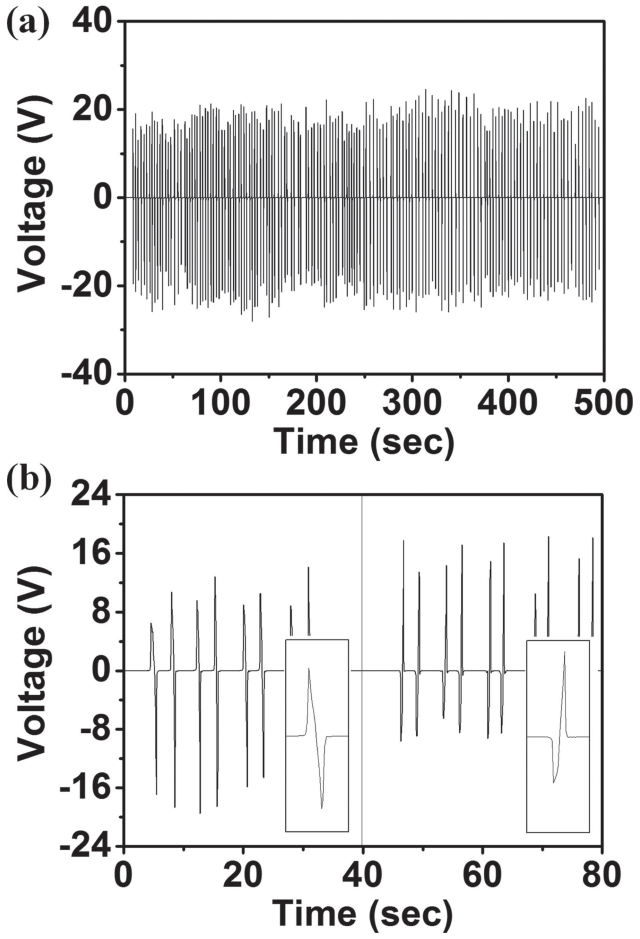

Figure 3. a) The stability and durability test of HP-NG, the output voltage of the $ZnSnO_3$:PDMS composite-based HP-NG driven by a vehicle tire. b) The polarity-switching tests under a rolling tire (forward and reverse connections) demonstrate that the output signals are from HP-NG rather than the instruments.

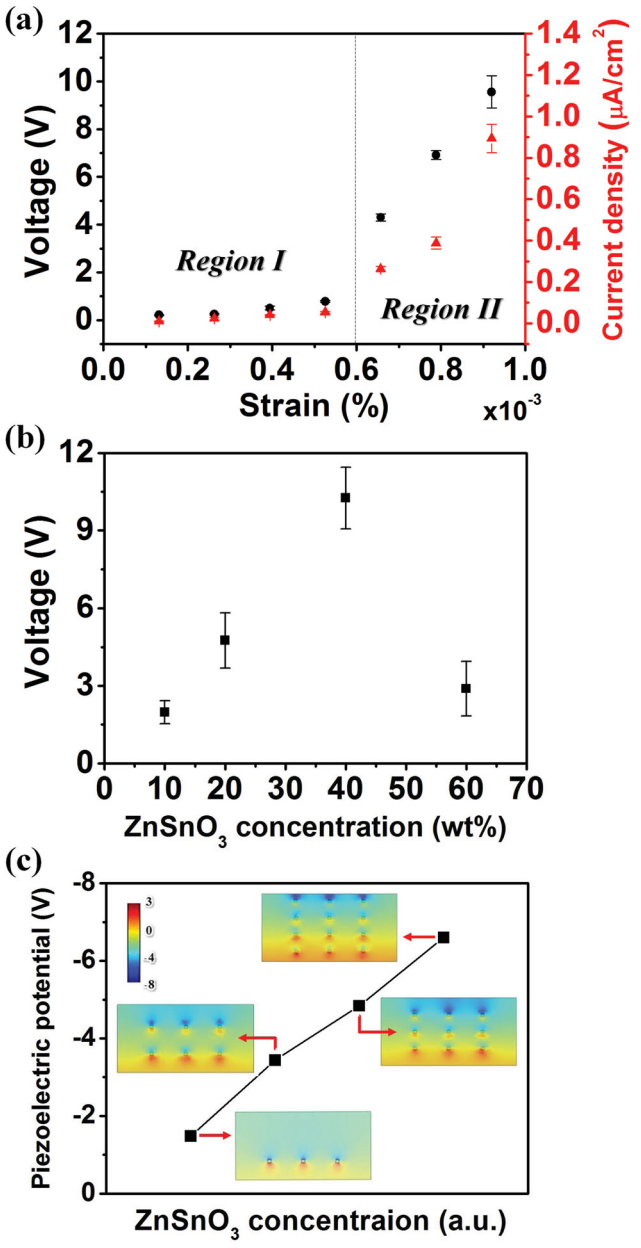

Figure 4. a) Output voltage and current density of $ZnSnO_3$:PDMS composite-based HP-NG (40 wt% $ZnSnO_3$) with different compressive forces. Little enhancement is observed in the output voltage and current at up to ≈0.52% strain (Region I), and abrupt enhancement in voltage and current is observed above 0.67% strain (Region II). b) The variation of output voltage from HP-NG with $ZnSnO_3$ concentration. c) COMSOL simulation results; output piezoelectric potential distribution of HP-NG with different $ZnSnO_3$ concentration.

HP-NG devices, for composite ratios of 10, 20, 40, and 60 wt%, respectively, under constant vertical strain of 0.91%, as shown in Figure 4b (the actual output voltage and current data are shown in the Supporting Information, Figure S6). It is clear that the piezoelectric voltage output initially increases with increasing $ZnSnO_3$ concentration up to 40 wt%, and reaches a maximum value of about 12 V. However, the piezoelectric voltage output starts to decrease for further increases in the $ZnSnO_3$ concentration, and reaches a lowest value of about 3 V. Further, the COMSOL package was used to investigate the piezoelectric potential distribution in the HP-NG as a function of the $ZnSnO_3$ nanocube density under vertical compression. It was found that with an increase in the amount of cubes, the piezoelectric potential increases linearly for the HP-NG system, as shown in the Figure 4c. These images depict the color-coded piezoelectric potential distributions with different numbers of $ZnSnO_3$ nanocubes embedded into the PDMS matrix. In simulations, the piezoelectric potential increased linearly with the piezoelectric nanocube density in the polymer matrix. In contrast, the experimentally obtained output voltage from an HP-NG with a high concentration of nanocubes (60 wt%) was low. This discrepancy will be discussed in detail in the next section. Furthermore, to confirm that the signals obtained were due to the piezoelectric nature of the $ZnSnO_3$ nanocubes, we measured the output signal from PDMS polymer with no $ZnSnO_3$ nanocubes. There was no distinct voltage or current outputs from the PDMS polymer under vertical compressive force.

The working mechanism of the composite-based HP-NGs was investigated. The working principle of the HP-NG is based on the piezoelectric properties of $ZnSnO_3$ nanocubes, and the creation of an inner piezoelectric field inside the $ZnSnO_3$ under an applied vertical compressive strain. Since $ZnSnO_3$ is a piezoelectric material with a space group of *R3c* due to its large polarization along the *c*-axis (≈59 μC cm^{-2}). Since, in the $ZnSnO_3$ structure, the displacement of the Zn ion is greater than that of the Sn ion along the *c*-axis because the displacement of the Zn ion in the ZnO_6 cluster is 0.5 Å, while that of the Sn ion in the SnO_6 cluster is 0.2 Å.[17] Therefore, a spontaneous polarization is generated along the *c*-axis, which is the source of piezoelectricity in this material.

To understand the working mechanism, the whole NG device can be considered as a capacitor for simplicity. Since the whole device acts as capacitor, charge-pumped electron flow is driven back and forth through an external circuit. The charging and discharging process results in alternating current (AC)-type charge generation by the HP-NG. In details, due to the piezoelectric/ferroelectric nature of the $ZnSnO_3$, the electric dipoles inside the $ZnSnO_3$ nanocubes are randomly oriented in the composite structure between the top and bottom electrode under no external force, which results in zero net dipole moment, leading no piezoelectric potential generation, as described in **Figure 5**a. When a small external vertical compressive force (strain below 0.52%) is applied, as shown Figure 5b, only minor potential is developed across the electrodes, which originates not from the piezoelectric behavior of $ZnSnO_3$, but from the change in the capacitance of device, because such small stress is not enough to produces significant strain to the $ZnSnO_3$ nanocubes. However, with the application of a larger vertical compressive force, the piezoelectric potential is generated inside the $ZnSnO_3$ abruptly, and the electric dipoles align strongly in a single direction due to stress-induced poling effect,[35–37] which creates a significant potential across the electrodes, as shown Figure 5c. In order to screen the piezoelectric potential, positive and negative charges are accumulated at the top and bottom electrodes, respectively, resulting in voltage and current output signals from the device. Further, when the vertical compressive force is released, the piezoelectric potential is diminished, and the accumulated charges move back to the opposite direction (Figure 5d). Therefore, continuous application and releasing of the compressive force results in AC-type voltage and current output signals from the HP-NG.

As discussed, with an increase of the $ZnSnO_3$ concentration in the PDMS polymer matrix, the output performance of the HP-NG increases and reaches a maximum value of 12 V under a vertical strain of 0.91% for 40 wt% $ZnSnO_3$. The higher output performance by the increase of the $ZnSnO_3$ concentration is mainly attributed to the high dielectric constant of the HP-NG, which arises due to interface polarization between the $ZnSnO_3$ nanocubes and the PDMS matrix. It is well known that interfaces in heterogeneous materials give rise to an interfacial or a Maxwell-Wagner-Sillars polarization, thus leading to an abrupt change of the total dielectric constant.[38–40] When the volume content of $ZnSnO_3$ reaches 40%, the filler–filler distance (between $ZnSnO_3$ nanocubes) becomes quite narrow. Thus, the dipole polarization between the $ZnSnO_3$ nanocubes is solidified, which leads to a rapid increase in the dielectric constant, resulting in high polarization. Therefore, we can obtain high voltage output from the HP-NG with 40 wt% $ZnSnO_3$ nanocubes. However, when the $ZnSnO_3$ amount is increased further and reaches up to 60 wt%, the insulation of the composites becomes weak, which leads to an electric breakdown, resulting in very low output voltage (60 wt%

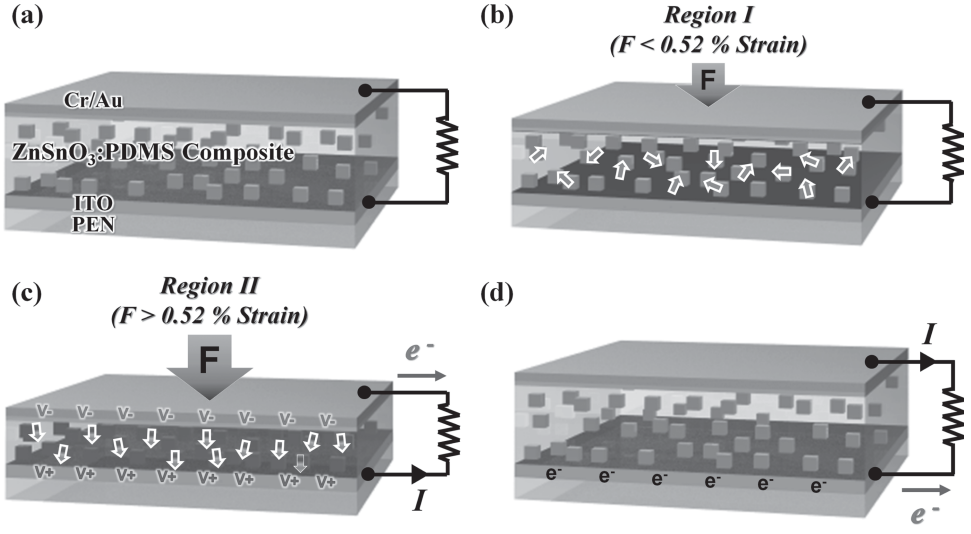

Figure 5. Proposed mechanism of the $ZnSnO_3$ nanocube:PDMS-based HP-NG. a) In the HP-NG, no signal is observed in the absence of external force. b) When a small external vertical force (strain ≈0.52%) is applied, only minor potential is developed across the electrodes due to capacitance change, and minute electric signals are observed, since significant strain on the piezoelectric $ZnSnO_3$ nanocube cannot be produced. c) When high vertical compressive force is applied to the HP-NG, the piezoelectric potential is created inside the nanocubes, which aligns the electric dipoles in a single direction (stress-induced poling), resulting in a flow of electrons. d) As the external force is removed, the piezoelectric potential disappeared, and the accumulated electrons flow back via the external circuit.

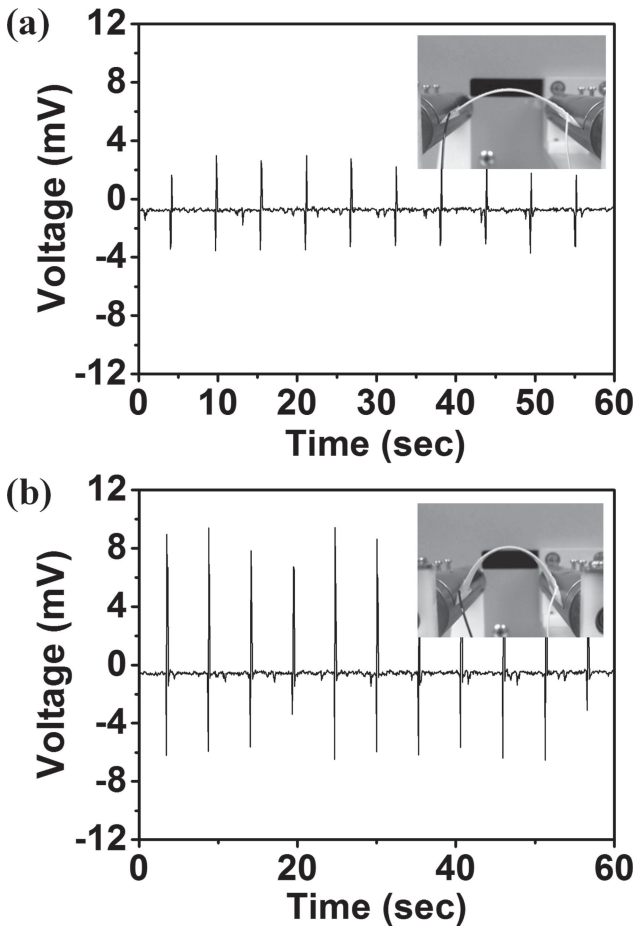

Figure 6. Output voltage of HP-NG under a) weak and b) strong bending conditions. Photograph of weak and strong bending of HP-NG are shown in insets of (a,b), respectively.

$ZnSnO_3$).[39,40] The discrepancy in experimental and simulation results (as shown in Figure 4b,c) is due to the different insulation resistance of the HP-NG devices with different $ZnSnO_3$ concentrations.

The piezoelectric power-generating performance of an HP-NG was also investigated under bending conditions. A weak piezoelectric signal (output voltage and current) was observed from the HP-NG in strong bending conditions, while no significant signal was detected under bending (**Figure 6**a,b). Nanocube/polymer composite-based HP-NG cannot experience significant strain under conditions of bending due to its composite structure in which most of stain is concentrated into the PDMS polymer matrix rather than the inorganic piezoelectric nanocubes. Further, the output voltage is closely related to alignment of dipoles. Thus, alignment of the dipoles in one direction without any electrical poling treatment is very difficult due to low applied strain to the $ZnSnO_3$ nanocubes embedded into the polymer matrix under bending. Hence, nanocube/polymer composite-based HP-NG can be effectively strained under conditions of applied vertical force, which generates large voltage and current output. This unique high unidirectionality of the power generation behavior from the HP-NGs even without electrical poling is desirable for large-scale piezoelectric power generation under vertical mechanical compression.

3. Conclusions

We have realized unidirectional, high-performance, lead-free, and flexible HP-NGs based on a composite of $ZnSnO_3$ nanocubes and PDMS without any treatment of electrical poling. The piezoelectric output voltage and current density reached high values of 20 V and 1 μA cm^{-2} under the motion of vehicle tires, which is the highest power generation performance achieved thus far by HP-NGs. The HP-NGs exhibit excellent robustness and durability, and can consistently harvest mechanical energy from environmental sources for an extended period. A series of HP-NGs with different $ZnSnO_3$ concentrations were was fabricated, and their electric output was measured under different vertical compressive forces. Furthermore, the HP-NG with 40 wt% $ZnSnO_3$ showed a maximum output voltage of up to 12 V and current density of up to 0.89 μA cm^{-2}, under 0.91% vertical compressive strain. The piezoelectric output voltage was found to increase with increasing $ZnSnO_3$ nanocube concentration up to 40 wt%, and then started to decrease. A corresponding working mechanism was proposed. The robustness and boosted electric output from the proposed HP-NGs provide a promising platform for harvesting energy from the motion of automobiles, and for biomedical applications. The devices also have great potential for transport monitoring applications, such as self-powered speed and pressure sensors.

4. Experimental Section

In a typical experiment for the synthesis of single-crystalline $ZnSnO_3$ nanocubes via an aqueous solution method, 2.88 g (10 mmol) of zinc sulfate heptahydrate ($ZnSO_4{\cdot}7H_2O$) were added into 100 mL of deionized (DI) water, and the solution was stirred at room temperature until the $ZnSO_4{\cdot}7H_2O$ was dissolved completely. Then, 2.67 g (10 mmol) of sodium stannate solution ($Na_2SnO_3{\cdot}3H_2O$) were poured into $ZnSO_4{\cdot}7H_2O$ solution, resulting in a 1:1 mol% molar ratio of $ZnSO_4{\cdot}7H_2O$ and $Na_2SnO_3{\cdot}3H_2O$. The mixed solution was vigorously stirred at 80 °C for five hours. After the reaction, the precipitates were collected by centrifugation and washed with DI water several times to remove residual ions in the products. The final products were then dried in air at 100 °C for one hour.

FE-SEM, EF-TEM (EM 912 Omega), XRD measurements were performed for the morphological and structural investigation of $ZnSnO_3$ nanostructure. The $ZnSnO_3$ nanocubes were homogeneously mixed with PDMS polymer. The well-mixed $ZnSnO_3$/PDMS was spin-coated onto ITO/PEN substrate. Thin films of Cr (10 nm) and Au (100 nm) were deposited sequentially onto the $ZnSnO_3$/PDMS layer by e-beam evaporation as a top electrode. A pushing tester (Z-tec Co., Ltd, model no. ZPS-100) was used to create strain in the HP-NGs. A Keithley 6485 picoammeter and a 2182A voltmeter were used to measure the low-noise output voltage and current generated by the HP-NGs, respectively.

Supporting Information

Supporting Information is available from the Wiley Online Library or from the author.

Acknowledgements

This work was financially supported by the National Research Foundation of Korea (NRF) grant funded by the Ministry of Education, Science and Technology (MEST) (2012R1A2A1A01002787, 2010-0019086, 2009-0083540) and the Energy International Collaboration Research & Development Program of the Korea Institute of Energy Technology Evaluation and Planning (KETEP) funded by the Ministry of Knowledge Economy (MKE) (2011-8520010050).

Received: April 23, 2013
Revised: May 30, 2013
Published online: July 5, 2013

[1] Y. Saito, H. Takao, T. Tani, T. Nonoyama, K. Takatori, T. Homma, T. Nagaya, M. Nakamura, *Nature* **2004**, *432*, 84.
[2] E. Cross, *Nature* **2004**, *432*, 24.
[3] Z. L. Wang, J. Song, *Science* **2006**, *312*, 242.
[4] G. Zhu, R. Yang, S. Wang, Z. L. Wang, *Nano Lett.* **2010**, *10*, 3151.
[5] M.-Y. Choi, D. Choi, M.-J. Jin, I. Kim, S.-H. Kim, J.-Y. Choi, S. Y. Lee, J. M. Kim, S.-W. Kim, *Adv. Mater.* **2009**, *21*, 2185.
[6] D. Choi, M.-Y. Choi, W. M. Choi, H.-J. Shin, H.-K. Park, J.-S. Seo, J. Park, S.-M. Yoon, S. J. Chae, Y. H. Lee, S.-W. Kim, J.-Y. Choi, S. Y. Lee, J. M. Kim, *Adv. Mater.* **2010**, *22*, 2187.
[7] S. N. Cha, J.-S. Seo, S. M. Kim, H. J. Kim, Y. J. Park, S.-W. Kim, J. M. Kim, *Adv. Mater.* **2010**, *22*, 4726.
[8] S. Xu, Y. Qin, C. Xu, Y. Wei, R. Yang, Z. L. Wang, *Nat. Nanotechnol.* **2010**, *5*, 366.
[9] Z. L. Wang, *Adv. Mater.* **2011**, *24*, 279.
[10] K. Y. Lee, B. Kumar, J.-S. Seo, K.-H. Kim, J. I. Sohn, S. N. Cha, D. Choi, Z. L. Wang, S.-W. Kim, *Nano Lett.* **2012**, *12*, 1959.
[11] B. Kumar, S.-W. Kim, *Nano Energy* **2012**, *1*, 342.
[12] H.-K. Park, K. Y. Lee, J.-S. Seo, J.-A Jeong, H.-K. Kim, D. Choi, S.-W. Kim, *Adv. Funct. Mater.* **2011**, *21*, 1187.
[13] T. T. Pham, K. Y. Lee, J.-H. Lee, K. H. Kim, K. S. Shin, M. K. Gupta, B. Kumar, S.-W. Kim, *Energy Environ. Sci.* **2013**, *6*, 841.
[14] P. K. Panda, *J. Mater. Sci.* **2009**, *44*, 5049.
[15] Z. Wang, J. Liu, F. Wang, S. Chen, H. Luo, X. Yu, *J. Phys. Chem. C* **2010**, *114*, 13577.
[16] J. Zhang, K. L. Yao, Z. L. Liu, G. Y. Gao, Z. Y. Sun, S. W. Fan, *Phys. Chem. Chem. Phys.* **2010**, *12*, 9197.
[17] Y. Inaguma, M. Yoshida, T. Katsumata, *J. Am. Chem. Soc.* **2008**, *130*, 6704.
[18] H. Ge, Y. Hou, C. Wang, M. Zhu, H. Yan, *Jpn. J. Appl. Phys.* **2009**, *48*, 041405.
[19] D. Corso, M. Posternak, R. Resta, A. Baldereschi, *Phys. Rev. B* **1994**, *50*, 10715.
[20] M.-C. Wang, F.-Y. Hsiao, C.-S. His, N.-C. Wu, *J. Cryst. Growth* **2002**, *246*, 78.
[21] D. Kovacheva, K. Petrov, *Solid State Ionics* **1998**, *109*, 327.
[22] X. Y. Xue, Y. J. Chen, Q. H. Li, C. Wang, Y. G. Wang, T. H. Wang, *Appl. Phys. Lett.* **2006**, *88*, 182102.
[23] B. Geng, C. Fang, F. Zhan, N. Yu, *Small* **2008**, *4*, 1337.
[24] W. B. Jackson, R. L. Hoffman, G. S. Herman, *Appl. Phys. Lett.* **2005**, *87*, 193503.
[25] Y. Zeng, T. Zhang, H. Fan, G. Lu, M. Kang, *Sens. Actuators, B* **2009**, *143*, 449.
[26] P. Görrn, F. Ghaffari, T. Riedl, W. Kowalsky, *Solid State Electron.* **2009**, *53*, 329.
[27] J. M. Wu, C. Xu, Y. Zhang, Z. L. Wang, *ACS Nano* **2012**, *6*, 4335.
[28] J. M. Wu, C. Xu, Y. Zhang, Ya Yang, Y. Zhou, Z. L. Wang, *Adv. Mater.* **2012**, *24*, 6094.
[29] Y. Hu, Y. Zhang, C. Xu, G. Zhu, Z. L. Wang, *Nano Lett.* **2010**, *10*, 5025.
[30] L. Lin, C.-H. Lai, Y. Hu, Y. Zhang, X. Wang, C. Xu, R. L Snyder, L.-J Chen, Z. L. Wang, *Nanotechnology* **2011**, *22*, 475401.
[31] K.-I. Park, M. Lee, Y. Liu, S. Moon, G.-T. Hwang, G. Zhu, J. E. Kim, S. O. Kim, D. K. Kim, Z. L. Wang, K. J. Lee, *Adv. Mater.* **2012**, *24*, 2999.
[32] Y. Yang, J. H. Jung, B. K. Yun, F. Zhang, K. C. Pradel, W. Guo, Z. L. Wang, *Adv. Mater.* **2012**, *24*, 5357.
[33] J. Jung, M. Lee, J.-I Hong, Y. Ding, C.-Y. Chen, L.-J. Chou, Z. L Wang, *ACS Nano* **2011**, *5*, 10041.
[34] N.-N. Ge, C.-M. Liu, Y. Cheng, X.-R. Chen, G.-F. Ji, *Phys. B* **2011**, *406*, 742.
[35] G. Luchaninov, A. V. Shil'nikov, L. A. Shuvalov, V. A. Malyshev, *Ferroelectrics* **1993**, *145*, 235.
[36] T. Kumazawa, Y. Kumagai, H. Miura, M. Kitano, K. Kushida, *Appl. Phys. Lett.* **1998**, *72*, 608.
[37] Gruverman, B. J. Rodriguez, A. I. Kingon, R. J. Nemanich, A. K. Tagantsev, J. S. Cross, M. Tsukada, *Appl. Phys. Lett.* **2003**, *83*, 728.
[38] D. Yang, L. Zhang, H. Liu, Y. Dong, Y. Yu, M. Tian, *J. Appl. Polym. Sci.* **2012**, *125*, 2196.
[39] M. Arous, H. Hammamia, M. Lagache, A. Kallel, *J. Non-Cryst. Solids* **2007**, *353*, 4428.
[40] H. Hammamia, M. Arous, M. Lagache, A. Kallel, *J. Alloys Compd.* **2007**, *430*, 1.